



Since January 2020 Elsevier has created a COVID-19 resource centre with free information in English and Mandarin on the novel coronavirus COVID-19. The COVID-19 resource centre is hosted on Elsevier Connect, the company's public news and information website.

Elsevier hereby grants permission to make all its COVID-19-related research that is available on the COVID-19 resource centre - including this research content - immediately available in PubMed Central and other publicly funded repositories, such as the WHO COVID database with rights for unrestricted research re-use and analyses in any form or by any means with acknowledgement of the original source. These permissions are granted for free by Elsevier for as long as the COVID-19 resource centre remains active.



# Assessing the efficacy of interventions to control indoor SARS-CoV-2 transmission: An agent-based modeling approach

Trevor S. Farthing, Cristina Lanzas\*

North Carolina State University, Raleigh, NC, USA

## ARTICLE INFO

### Keywords:

Aerosol  
Agent-based model  
COVID-19  
Droplet  
Indoor transmission  
SARS-CoV-2

## ABSTRACT

Nonpharmaceutical interventions for minimizing indoor SARS-CoV-2 transmission continue to be critical tools for protecting susceptible individuals from infection, even as effective vaccines are produced and distributed globally. We developed a spatially-explicit agent-based model for simulating indoor respiratory pathogen transmission during discrete events taking place in a single room within a sub-day time frame, and used it to compare effects of four interventions on reducing secondary SARS-CoV-2 attack rates during a superspreading event by simulating a well-known case study. We found that preventing people from moving within the simulated room and efficacious mask usage appear to have the greatest effects on reducing infection risk, but multiple concurrent interventions are required to minimize the proportion of susceptible individuals infected. Social distancing had little effect on reducing transmission if individuals were randomly relocated within the room to simulate activity-related movements during the gathering. Furthermore, our results suggest that there is potential for ventilation airflow to expose susceptible people to aerosolized pathogens even if they are relatively far from infectious individuals. Maximizing the vertical aerosol removal rate is paramount to successful transmission-risk reduction when using ventilation systems as intervention tools.

## 1. Introduction

Understanding transmission mechanisms is necessary to generate evidence-based guidance for controlling infectious diseases. Severe Acute Respiratory Syndrome Coronavirus 2 (SARS-CoV-2), the causative agent of Coronavirus Disease 2019 (COVID-19), is primarily spread through infectious respiratory droplets and aerosols of varying size (CDC, 2021). These media are expelled when an individual speaks, coughs, sneezes, or otherwise expectorates (Atkinson et al., 2009; Stadnytskyi et al., 2020). Pathogen transmission can occur when these virion-containing particles are inhaled by, or otherwise come into contact with the mucosae or conjunctiva (i.e., mouth, nasal membranes, or eyes) of a susceptible person (WHO, 2020). Aerosol transmission has proven to be an important transmission pathway, particularly for large clusters associated with superspreading events (Hammer et al., 2020; Qian et al., 2020; Leclerc et al., 2020; Park et al., 2020; Wang et al., 2021).

Transmission of SARS-CoV-2 is more likely in indoor settings than outdoors (Qian et al., 2020; Leclerc et al., 2020). Households are the

most common venue linked to transmission, but healthcare facilities, religious venues, food processing plants or prisons are also likely to be associated with large clusters of COVID-19 cases (Leclerc et al., 2020). Recommended nonpharmaceutical interventions to reduce indoor transmission include: social distancing, use of face coverings, increased ventilation, and reduced group sizes (CDC, 2021).

Some mathematical models have been built to support individual-level risk assessment of indoor transmission and analyze aerosol contributions to past outbreaks. Chande et al. (2020) created a tool to assess the U.S. County level probability that someone infected with SARS-CoV-2 will attend events of varied sizes. Their tool is useful for estimating the probability that SARS-CoV-2 transmission could occur during any gathering, but provides no direct measure of transmission risk from infectious individuals during events and no way to assess the impact of intervention strategies other than reducing group sizes. Other models have sought to determine the role that aerosolized infectious droplets play in indoor SARS transmission relative to larger droplets that are unlikely to be inhaled, and quantify the transmission risk attributable to aerosols in varied environments (Bhagat et al., 2020; Chen et al.,

*Abbreviations:* ABM, Agent-based model; SARS-CoV-2, Severe Acute Respiratory Syndrome Coronavirus 2; COVID-19, Coronavirus Disease 2019.

\* Correspondence to: 1051 William Moore Dr., RB410, Raleigh, NC 27606, USA.

*E-mail address:* [clanzas@ncsu.edu](mailto:clanzas@ncsu.edu) (C. Lanzas).

<https://doi.org/10.1016/j.epidem.2021.100524>

Received 6 February 2021; Received in revised form 5 October 2021; Accepted 11 November 2021

Available online 12 November 2021

1755-4365/© 2021 The Authors.

Published by Elsevier B.V. This is an open access article under the CC BY-NC-ND license

(<http://creativecommons.org/licenses/by-nc-nd/4.0/>).

2020; Lelieveld et al., 2020; Miller et al., 2020; Sun and Zhai, 2020). These models are primarily based on Wells-Riley equations for estimating aerosol-attributable risk, which assume homogenous spatio-temporal mixing of air constituents and exposure to infectious agents (Riley et al., 1978). Mathematical indices and parameter values in these models can be adjusted to simulate effects of intervention strategies like social distancing (Sun and Zhai, 2020) and increased ventilation rates (Bhagat et al., 2020; Lelieveld et al., 2020; Miller et al., 2020; Sun and Zhai, 2020), but are insufficient for capturing or accounting for any behavior- or environment-mediated spatiotemporal heterogeneity in transmission risk. Shao et al. (2021) used a fluid dynamics model to simulate ventilation effects on SARS-CoV-2 transmission while allowing for heterogenous droplet movement behaviors. Their findings highlight the need to account for within-room spatial heterogeneity when studying indoor transmission risk, as phenomena like ventilation can increase infection risk to individuals in one area of a room or building while simultaneously mitigating risk in another.

Here, we present a spatially-explicit agent-based model (ABM) for simulating within-room respiratory pathogen transmission to inform policy-making decisions aiming to mitigate indoor transmission and implementing individual-level nonpharmaceutical interventions. By simulating spatiotemporal droplet dynamics (e.g., emission of varying droplet size and subsequent distribution in the environment) as well as allowing for dynamic movement and positioning of infectious and susceptible individuals, our model allows virion exposure rates to vary

within indoor settings. We use our model to estimate effects of proposed COVID-19 intervention strategies for indoor environments (i.e., increased airflow, limiting contact durations, wearing masks, and increased interpersonal spacing). For benchmarking purposes, we simulate the outbreak that took place during a choir practice in Skagit County, WA in March 2020 (Hamner et al., 2020). This event was characterized by the spread of an early SARS-CoV-2 variant from one infectious person to 53 susceptible individuals during the 150-min rehearsal (Hamner et al., 2020), and is a well-documented case study on SARS-CoV-2 superspreading within in a fully susceptible population at an indoor gathering. Additionally, we further investigate potential drivers of superspreading events, like the Skagit County example, by characterizing and comparing how different aspects of indoor gatherings (i.e., population density, duration, quanta production by infectious individuals, and ventilation effects) impact transmission risk. Through these analyses we provide guidance for minimizing SARS-CoV-2 transmission during indoor gatherings.

## 2. Methods

### 2.1. Model Description

We developed a spatially-explicit, stochastic ABM to simulate both direct-droplet and airborne respiratory pathogen transmission in indoor settings. This model was created and executed using the open-source

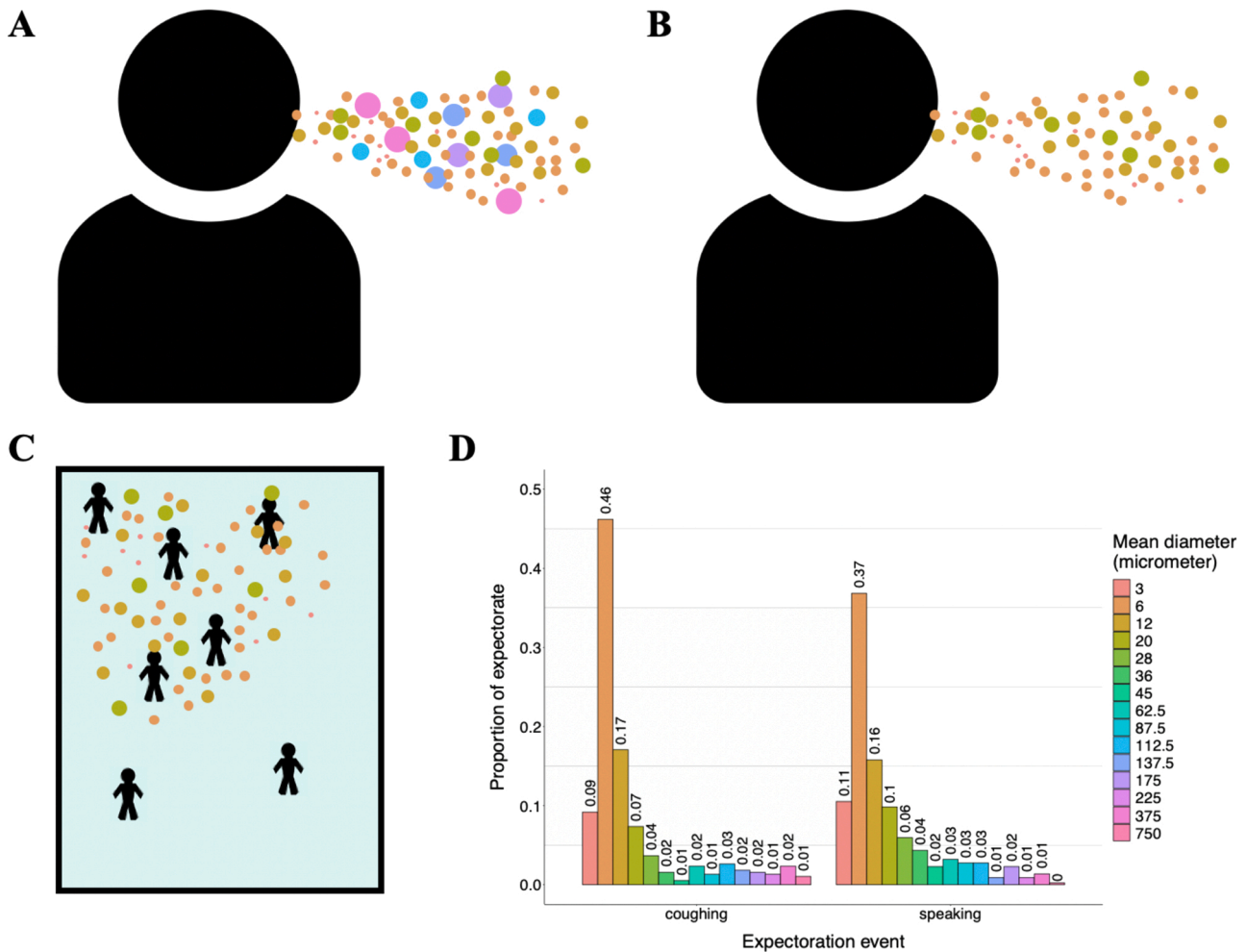


Fig. 1. Model droplet dynamics. A) Infectious individuals expel droplets of different sizes. B) Relatively large droplets fall out of the air quickly post expectoration. C) Smaller droplets remain aerosolized for longer time periods and move throughout the simulated room via diffusion and forced airflow effects. D) Distribution of droplet sizes during expectoration events. Distributions of size classes during coughing and speaking events are based on findings of Chao et al. (2009), and represent mean observed droplet-size measurements they recorded 60 mm away from individuals' mouths immediately following these activities.

modeling software, NetLogo (Ver. 6. 1. 1 – Wilensky, 1999) and is available for download at <https://github.com/lanzaslab/droplet-ABM>. In [Supplemental Materials 1](#) we provide a detailed description of our model in accordance with standards outlined by (Grimm et al., 2020). We present a limited summary of the model design below. When describing infectious media in our model, we use the term “droplet” to refer to respiratory droplets of any size.

Agents in our model represent people congregating in a fixed space (e.g., students in a classroom, diners in a restaurant, etc.). Patches (i.e., grid cells in the NetLogo model interface) represent  $1 \times 1 \text{ m}^2$  areas, and the spatial extent can range from 1 to  $\infty \text{ m}^2$ . The model time step is 1 min. Droplets ranging from 3 to  $750 \mu\text{m}$  in diameter are expelled by infectious agents (Fig. 1A). Subsequently, droplets can be inhaled, fall out, diffuse to nearby patches, move via directed airflow, and decay at fixed rates over the course of a simulation. Infection in our model is driven by exposure to virions contained in these droplets, and the number of virions per droplet scales with droplet size. The rate at which droplets fall out (i.e., are removed from circulating air flows) of the simulation is based on the calculated terminal velocity falling speed for droplets, and therefore varies with droplet size (Fig. 1B). Droplet sizes incapable of settling on the ground within one minute are allowed to move between patches via ventilation- and diffusion-induced airflow (Fig. 1C). Thus, risk of exposure and subsequent infection for susceptible individuals varies by space and time during the simulation. We recognize that the ability of forced air ventilation systems to reduce local respiratory pathogen transmission is linked to their ability to move aerosolized droplets away from susceptible individuals in three dimensions (Bhagat et al., 2020; Shao et al., 2021). Though this effect is not explicitly tied to airflow inputs in our model, which only allows airflow in two dimensions, we can effectively simulate ventilation-induced aerosolized droplet movement to heights outside of individuals’ inhalation ranges by increasing the decay rate when ventilation effects are simulated. In addition to controlling the number of individuals present and the size of the simulated world, users can dictate infectiousness parameters and other scenario-specific variable values (e.g., number of infectious individuals, probability that infectious individuals are asymptomatic, cough frequency, number virions per mL of droplet fluid, risk of infection given exposure to 1 virion, etc.), ventilation parameters (e.g., direction and speed of airflow, droplet filtration probability, etc.), and adherence to transmission-risk-reduction guidelines (e.g., mask usage, local social distancing, etc.).

This ABM is intended to simulate pathogen transmission during events lasting  $< 1$  day. The underlying transmission model is based on a Susceptible-Exposed-Infectious-Recovered (SEIR) framework, but due to the limited duration of simulations we make the assumption that no individuals exist long enough to exceed pathogen latent or infectious periods.

## 2.2. Testing SARS-CoV-2 transmission reduction strategies

### 2.2.1. Case scenario and model inputs

In March 2020, there was a probable SARS-CoV-2 superspreading event during a choir practice taking place at a church in Skagit County, Washington, USA (Hamner et al., 2020). Sixty-one people were in attendance, one attendee was experiencing flu-like symptoms at the time and later tested positive for COVID-19 (Hamner et al., 2020). This individual likely infected 53 other attendees over the course of the event (Hamner et al., 2020). We describe our rationale for setting scenario-specific input values to simulate this case in our model below, with additional details given in [Supplemental Materials 2](#). [Supplemental Materials 3](#) describes how sensitive simulated infection risk is to variations in select model parameters.

Because this superspreading event is thought to be the result of transmission from a single infectious individual (Hamner et al., 2020), all simulations contained only one infectious person. The infectious person was assumed to be symptomatic during the choir practice. We assumed all droplets were expelled from this individual at a height of 1.7 m, the approximate mean height of U.S. adults (Fryar et al., 2018).

We make the assumption that the cough frequency for a symptomatic COVID-19 patient is equal to that of individuals with a chronic cough condition. Therefore, every minute our infectious individual had a 19% probability to expel droplets through coughing (Lee et al., 2012), and an 81% chance to expel droplets through an unspecified other activity (e.g., speaking, singing, etc.). Using the procedure described by Railsback and Grimm (2011), droplet travel distances for coughing and non-coughing expectoration events were randomly drawn from log-normal distributions with known means and standard deviations. Travel distances for coughing events were drawn from a distribution with a mean of 5 m and standard deviation of 0.256 m (Bourouiba et al., 2014). Travel distances for non-coughing events were drawn from a distribution with a mean of 0.55 m and standard deviation of 0.068 m (Das et al., 2020). The angle of droplet spread during coughing and non-coughing expectorations were  $35^\circ$  and  $63.5^\circ$ , respectively, in accordance with median values of mouth-angle ranges described by Kwon et al. (2012). We calibrated the risk of infection for susceptible individuals given exposure droplets expelled by the simulated infectious person, and the number of droplets expelled by this person to reflect the estimated infectiousness of the symptomatic individual in the case study using linear regression methods described in [Appendix S2](#). We set the inhalation rate for simulated individuals to  $0.023 \text{ m}^3 \text{ air/min}$ , a rate consistent with adults participating in light activity (Adams, 1993).

We know from the Hamner et al. (2020) case report that the choir practice lasted 150 min in total, split into 4 distinct time intervals lasting 40, 50, 15, and 45 min. During the first time interval, all 61 attendees practiced together in the  $180 \text{ m}^2$  main hall for 40 min. In the second interval, the group split into two subsets of unspecified sizes. One subset rearranged themselves within the main hall, and the second subset moved into a separate room. The subsets rehearsed separately for 50 min. The third time interval was a 15-min break period when individuals mixed freely. During the final time interval, all attendees returned to the main hall to practice as a single group once more for 45 min. When practicing as single group during intervals 1 and 4, individuals sat in assigned seats (Miller et al., 2020) with chairs spaced 15.24–25.4 cm apart (Hamner et al., 2020). In our simulations, we decided to rearrange agents in our model after 40, 90, and 105 min to recreate mixing associated with changing time intervals. At timestep 105, individuals moved back to their initial placements, representing their adherence to assigned seating during interval 4 (i.e., minutes 105–150). The seating chart has not been shared due to privacy concerns (Miller et al., 2020) however, from the spacing estimate we can assume that a maximum of 2 people could be within  $1\text{-m}^2$  patches in our model scenario. Our ability to simulate mixing rates during specific time intervals was limited to this extent because we do not know specific seating arrangements, subset size or configuration, secondary room size, or interaction rates during the break period.

We assume that airborne droplets naturally diffuse throughout the simulated environment at a fixed rate of  $1.5\text{e}^{-3} \text{ m}^3/\text{min}$  (Castillo and Weibel, 2018) regardless of size, and decay at a rate of  $1.05\%/\text{min}$  (van Doremalen et al., 2020). Additionally, we know that the ventilation system in the main hall of the church consists of three supply vents that push a mixture of outdoor and recirculated air towards a single return vent on the opposite wall, though the true direction of forced airflow (e.g., North to South) is unclear from reports (Miller et al., 2020). Because it is uncertain whether or not the forced-air system was turned on during the choir practice (Miller et al., 2020), however, we decided to run our simulations in two sets: ventilation-on (i.e., both forced-air effects and natural diffusion moved droplets between patches) and ventilation-off (i.e., only natural diffusion moved droplets between patches). In the ventilation-on set, we additionally assume that droplets move from supply vents towards the return vent at a fixed rate of  $0.043\%/\text{min}$  (Miller et al., 2020), and that 90% of droplets were filtered prior to recirculation (Miller et al., 2020). Because we do not know the true direction of forced airflow, we simulated both North-to-South and East-to-West forced airflow movement in the ventilation-on set (Fig. 2).

In addition to modeling the baseline scenario, we modulated values of inputs related to group-level nonpharmaceutical intervention strategies (i.e., limited population, limited contact durations, mask usage, and meter-level social distancing) between simulations in order to assess the efficacy of each strategy on reducing the number of susceptible individuals infected. Regarding mask usage, we assumed face coverings have both source-prevention and wearer-protection effects, and reduced global droplet exposure/exhalation rates by 0%, 25%, 50%, 75% and 90%. The upper range here is intended to simulate the use of N95 and simple surgical masks, which are estimated to reduce aerosol emission rates by approximately 90% and 74%, respectively (Jefferson et al., 2008; Asadi et al., 2020). Lower values are intended to simulate the use of single- and multi-layered fabric masks, for which a wide range of aerosol-filtration efficacies have been reported (O'Kelly et al., 2020). When simulating mask usage, we assumed that all individuals were wearing masks and that all masks had the same efficacy. Table 1 outlines the model input values for our superspreading-scenario simulations.

### 2.2.2. Running simulations and analyses

We set up a factorial simulation run within the NetLogo BehaviorSpace using our specified input levels. We ran 1000 replicates of all input set combinations, ultimately resulting in 1,080,000 simulations. Simulations were aggregated into a single data set prior to analysis.

We used a beta regression model with a fixed unknown precision parameter,  $\phi$ , (Ferrari and Cribari-Neto, 2004) to estimate effects of interventions on the mean proportion of susceptible individuals infected in our full simulation set,  $\mu$ . Beta regression models are employed to analyze proportion data (Ferrari and Cribari-Neto, 2004; Cribari-Neto and Zeileis, 2010). We chose to use this method because the potential number of infected individuals in each simulation was limited by the simulated group size, which was a predictor variable of interest, and because preliminary analysis suggested that fitting our data to a beta distribution better explained observed variation than other regression models. We therefore determined it was more appropriate to evaluate effect sizes in terms of the relative proportion of susceptible people infected rather than their total number. We fit our data to the model:

$$\ln\left(\frac{\mu}{1-\mu}\right) = \beta_0 + \beta_1(\text{Gathering duration}) + \beta_2(\text{Mask use}) \\ + \beta_3(\text{Mask efficacy}) + \beta_4(\text{Group size}) + \beta_5(\text{Social distancing}) \\ + \beta_6(\text{Ventilation}) + \beta_7(\text{Movement}) + \beta_8(\text{Mask use} * \text{Group size}) \\ + \beta_9(\text{Mask use} * \text{Social distancing}) \\ + \beta_{10}(\text{Group size} * \text{Social distancing}) \\ + \beta_{11}(\text{Mask use} * \text{Group size} * \text{Social distancing}),$$

where *Gathering duration*, *Mask efficacy*, and *Group size* are intervention-strategy variables relating to: minutes of simulated interaction between

individuals, the efficacy of worn face masks for reducing expectoration and inhalation of infectious droplets, the simulated population size, and attempted meter-level social distancing in each realized simulation, respectively. The variables *Mask use*, *Movement*, and *Ventilation* are known confounders related to: reduced droplet spread distance from expectorating infectious individuals wearing masks, the number of times individuals were rearranged within simulations to reflect mixing of event attendees, and movement of infectious aerosols throughout the simulated space due to a forced-air ventilation system, respectively. *Mask use* is a binary variable taking the value of 1 when simulated individuals are masked (i.e., *Mask efficacy* > 0), and 0 when they are not. *Movement* takes any one value within the range of 1-to-4, dependent on *Gathering duration*. *Ventilation* is a binary variable taking the value of 1 for simulations in the “ventilation-on” subset, and 0 for those in the “ventilation-off” subset. Because we used a logit link function to fit this model,  $\beta$  estimates represent the additive effect of 1-unit increases in associated predictor variables on the log-odds of the susceptible population proportion infected, and the mean proportion of susceptible individuals infected for any given parameter space  $i$  can be calculated using the equation  $\mu_i = \frac{e^{x_i^T \beta}}{1 + e^{x_i^T \beta}}$  (Ferrari and Cribari-Neto, 2004).

Because beta regression procedures assume all dependent variable values fall between 0 and 1, we used the data transformation procedure described by (Cribari-Neto and Zeileis, 2010) to reconstruct our proportion data without these extremities. All analysis and plotting was carried out using functions from the “betareg” R package (Ferrari and Cribari-Neto, 2004) in RStudio (v. 1.1.463, RStudio Team, Boston, MA) (RStudio Team, 2018) running R (v. 3.6.2, R Foundation for Statistical Computing, Vienna, Austria) (R Core Team, 2020). We calculated a pseudo- $R^2$  (Ferrari and Cribari-Neto, 2004) to assess goodness of fit for our regression model.

### 2.3. Evaluating drivers of transmission in indoor gatherings

To assess the relative contribution of environmental conditions to SARS-CoV-2 transmission risk, we conducted a sensitivity analysis to ascertain relative effects of population density, gathering duration, quanta production by infectious individuals, and ventilation on SARS-CoV-2 infection risk beyond the conditions tested in the Skagit County case. In addition, we quantified the ability of different ventilation system aspects (i.e., air-change rate, filtration rate, and effective three-dimensional droplet removal rate) to reduce SARS-CoV-2 transmission risk. Table 2 describes the model input values for these indoor-gathering-risk-assessment simulations.

We set up a factorial simulation run within the NetLogo BehaviorSpace using our specified input levels. We ran 1000 replicates of each parameter set combination when the *Forced air* parameter was set to “on” and when it was “off.” We ran these sets separately in order to save

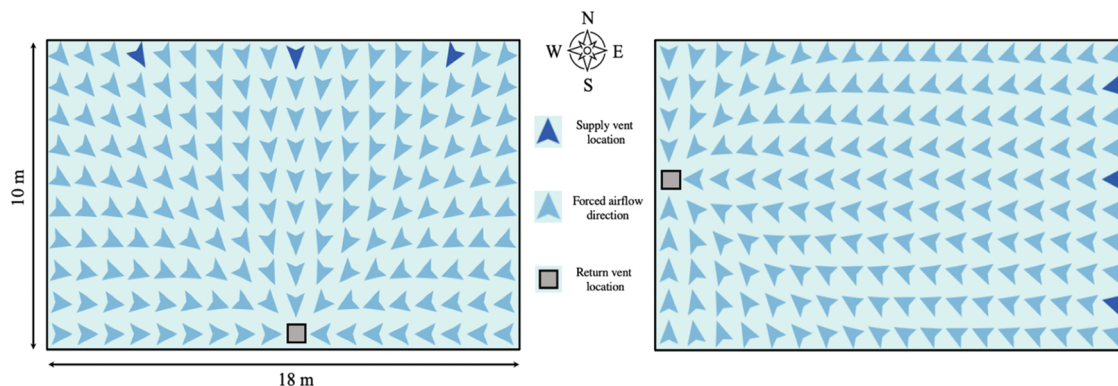


Fig. 2. Airborne infectious droplets in North-to-South and East-to-West forced airflow schemas have different maximum travel distances due to the shape of the simulated world.

**Table 1**

Parameter descriptions for simulations of the Skagit County, WA March 2020 SARS-CoV-2 transmission case study. \*Simulated worlds were 10 m × 18 m. †Standard deviations are given in parentheses. ‡Zero-percent mask efficacy is equivalent to no mask use. §Das et al. (2020) estimated the average travel distance of a 100-micrometer droplet expelled from a height of 1.7 m at a velocity of 0.5 m/s to be 0.55 m. They also found that the majority of 100-µm droplets will fall 0.55–2.35 m away from the expelling individual, depending on initial velocity, but droplets may settle up to 3.2 m away very rarely. a random draw of 10,000,000 samples from a log-normal distribution parameterized using 1.7-m and 0.2095-m droplet spread distance mean and standard deviation values, respectively, generated a distribution in line with this finding. The standard deviation we use in simulations for non-coughing expectoration is proportionate to the one used in this random draw.

Parameter/Model Input	Value (s)	Reference (s)
<i>Infectiousness parameters</i>		
Cough frequency (coughs/min)	0.19	Lee et al., 2012
Droplet count (droplets/expectoration)	9.7e <sup>5</sup> (3.9e <sup>5</sup> ) <sup>†</sup>	Miller et al., 2020, Appendix S2
Droplet spread angle – coughing (°)	35	Kwon et al., 2012
Droplet spread angle – not coughing (°)	63.5	Kwon et al., 2012
Droplet travel distance – coughing (m)	5 (0.256) <sup>†</sup>	Bourouiba et al., 2014
Droplet travel distance – not coughing (m)	0.55 (0.068) <sup>‡§</sup>	Das et al., 2020
<i>Scenario environment and individual behavior inputs</i>		
Area (m <sup>2</sup> )	180*	Hamner et al., 2020
Expectoration height (m)	1.7	Fryar et al., 2018
Inhalation rate (m <sup>3</sup> air/min)	0.023	Adams, 1993
Maximum people in a single 1-m <sup>2</sup> patch (people)	2	Hamner et al., 2020
Number of symptomatic individuals (people)	1	Hamner et al., 2020
<i>Scenario virion behavior inputs</i>		
Virion count (virions/mL fluid)	2.35e <sup>9</sup>	Wölfel et al., 2020
Virion decay rate (%/min)	1.05	van Doremalen et al., 2020
Virion infection risk (%/inhaled virion)	6.24	Appendix S2
<i>Scenario airflow inputs</i>		
Diffusion rate (m <sup>3</sup> /min)	1.5e <sup>-3</sup>	Castillo and Weibel, 2018
Forced air	on, off	–
Forced air direction	North-to-South, East-to-West	–
Air change rate (%/min)	4.3	Miller et al., 2020
Re-circulated air filtration (%/min)	90	Miller et al., 2020
<i>Scenario intervention inputs</i>		
Attempted social distancing (m)	0, 1, 2, 3	–
Contact duration (min)	20, 40, 60, 90, 105, 150	–
Mask efficacy (%)	0 <sup>‡</sup> , 25, 50, 75, 90	Jefferson et al., 2008; Asadi et al., 2020
Population (people)	10, 50, 61	–

computation time as there were many inputs that only changed when forced airflow was simulated. Ultimately, we produced 144,000 “off” simulations, and 20,160,000 “on” simulations. In both sets, we identified simulations when transmission occurred (i.e., simulations where ≥ 1 susceptible person was infected), and recorded this occurrence as the binary variable  $y_i$  so that

$$y_i = \begin{cases} 1 & \text{if transmission was observed} \\ 0 & \text{if no transmission occurred} \end{cases}$$

for each realized simulation,  $i$ .

We aggregated simulation data into a single data set and carried out a logistic regression analysis to estimate effects of variable inputs on observed differences in the probability of observing ≥ 1 infections. We chose to use a logistic regression here instead of another beta regression to simplify the interpretability of our results. Though we lose the ability

**Table 2**

Parameter descriptions for ventilation-system effect evaluations. \*All simulated worlds were square-shaped. †Based on linear modeling described in Appendix S2, these values equate to 1 (SD = 0) and 970 (SD = 390) quanta/hr. ‡Standard deviations are given in parentheses. §Das et al. (2020) estimated the average travel distance of a 100-micrometer droplet expelled from a height of 1.7 m at a velocity of 0.5 m/s to be 0.55 m. They also found that the majority of 100-µm droplets will fall 0.55–2.35 m away from the expelling individual, depending on initial velocity, but droplets may settle up to 3.2 m away very rarely. a random draw of 10,000,000 samples from a log-normal distribution parameterized using 1.7-m and 0.2095-m droplet spread distance mean and standard deviation values, respectively, generated a distribution in line with this finding. The standard deviation we use in simulations for non-coughing expectoration is proportionate to the one used in this random draw. ¶These parameter values were only used when the *Forced air* parameter value was set to “on.” #These parameter values were only used when the *Forced air* parameter value was set to “off.” \*\*All patches on the east side of the simulated world acted as supply vents. All patches on the west side acted as return vents. ††Zero-percent mask efficacy is equivalent to no mask use. †††Instead of specifying a fixed number of individuals in simulations, we scaled the simulated population with world size.

Parameter/Model Input	Value (s)	Reference (s)
<i>Infectiousness parameters</i>		
Cough frequency (coughs/min)	0.19	Lee et al., 2012
Droplet count (droplets/expectoration) <sup>†</sup>	1000 (0) <sup>‡</sup> , 9.7e <sup>5</sup> (3.9e <sup>5</sup> ) <sup>‡</sup>	Miller et al., 2020, Appendix S2
Droplet spread angle – coughing (°)	35	Kwon et al., 2012
Droplet spread angle – not coughing (°)	63.5	Kwon et al., 2012
Droplet travel distance – coughing (m)	5 (0.256) <sup>‡</sup>	Bourouiba et al., 2014
Droplet travel distance – not coughing (m)	0.55 (0.068) <sup>‡§</sup>	Das et al., 2020
<i>Scenario environment and individual behavior inputs</i>		
Area (m <sup>2</sup> )*	9, 36, 81	–
Expectoration height (m)	1.7	Fryar et al., 2018
Inhalation rate (m <sup>3</sup> air/min)	0.023	Adams, 1993
Maximum people in a single 1-m <sup>2</sup> patch (people)	2	Hamner et al., 2020
Number of infectious individuals (people)	1	–
Proportion of infectious individuals that are symptomatic (%)	0, 100	–
<i>Scenario virion behavior inputs</i>		
Virion count (virions/mL fluid)	2.35e <sup>9</sup>	Wölfel et al., 2020
Virion decay rate (%/min)	1.05, 5 <sup>¶</sup> , 10 <sup>¶</sup> , 25 <sup>¶</sup> , 50 <sup>¶</sup> , 75 <sup>¶</sup> , 90 <sup>¶</sup>	van Doremalen et al., 2020
Virion infection risk (%/inhaled virion)	6.24	Appendix S2
<i>Scenario airflow inputs</i>		
Diffusion rate (m <sup>3</sup> /min)	1.5e <sup>-3</sup>	Castillo and Weibel, 2018
Forced air	on, off	–
Forced air direction**	East-to-West	–
Air change rate (%/min)	0 <sup>#</sup> , 1 <sup>#</sup> , 5 <sup>#</sup> , 10 <sup>#</sup> , 25 <sup>#</sup> , 50 <sup>#</sup>	–
Re-circulated air filtration (%/min)	0 <sup>#</sup> , 1 <sup>#</sup> , 5 <sup>#</sup> , 90 <sup>#</sup> , 100 <sup>#</sup>	–
<i>Scenario intervention inputs</i>		
Attempted social distancing (m)	0	–
Contact duration (min)	10, 30, 60	–
Mask efficacy (%)	0 <sup>††</sup>	–
Population density (people/m <sup>2</sup> ) <sup>†††</sup>	0.333, 0.667, 1, 1.667	–

to comment on mean attack rates, we can still estimate environmental effects on transmission risk using a logistic regression. We fit our data to the model:

$$\ln \left( \frac{\Pr(y_i = 1)}{\Pr(y_i = 0)} \right) = \beta_0 + \beta_1(\text{Population density}) + \beta_2(\text{Gathering duration}) + \beta_3(\text{Quanta per hour}) + \beta_4(\text{Excess droplet removal rate}) + \beta_5(\text{Air change rate}) + \beta_6(\text{Air filtration rate}),$$

where *Population density* is given by  $\frac{n}{m^2}$ , and the *Excess droplet removal*

rate (%/min) represents the increased removal of aerosols due to ventilation-induced 3-dimensional droplet movement. It is given by the equation: (*Virion decay rate* – 1.05). The 1.05 here represents the general SARS-CoV-2 decay rate (i.e., 1.05%/min) as reported by (van Dorimalen et al., 2020). Subtracting this baseline value from the simulated Virion decay rate gives us an excess removal rate that we use as a proxy for 3-dimensional droplet removal attributable to forced airflow movement. When no forced airflow is simulated, excess droplet removal, air change, and filtration rates all equal 0. We calculated the Tjur (2009) pseudo- $R^2$  for our logistic regression model to assess goodness of fit.

### 3. Results and discussion

We developed a stochastic and spatially-explicit ABM for studying indoor individual-level respiratory pathogen transmission, and used it to demonstrate the potential effectiveness of multiple intervention strategies for reducing SARS-CoV-2 transmission in an indoor group setting mimicking that of a known superspreading event. We were able to effectively recreate the empirical proportion of susceptible individuals likely infected during the Skagit County superspreading event by simulating the gathering without implementing any intervention strategies (Fig. 3).

Our beta regression model for estimating intervention efficacy had a pseudo- $R^2$  of  $\approx 0.43$ . Given the number of stochastic processes in our ABM, the explanatory power of the model is acceptable. As shown in Fig. 4, duration limits and efficacious mask usage appear to have the greatest effects on reducing the proportion of susceptible individuals infected, but multiple concurrent interventions are required to minimize the proportion of susceptible individuals infected (Table 3, Fig. 4). However, it is important to note that observed proportional differences are more meaningful for relatively large groups than for smaller ones, as demonstrated by the positive  $\beta$  estimates for interaction terms including

the *Group size* variable (Table 3). The effectiveness of limiting the duration of gatherings for reducing the proportion of infected individuals appears to largely result from reducing the confounding movement effect that increases over time, thereby reducing the probability that susceptible individuals will move from uncontaminated space to areas with greater concentrations of infectious aerosols or nearby to infectious individuals where they may be exposed to large virion-containing droplets (Table 3). The regression model suggests that the effect of each random relocation event on the log-odds of the susceptible population proportion infected is  $\approx 41$  times that of each passing minute in the simulation (Table 3). We show that simply by limiting the time spent rehearsing in our simulations to 40 min, minimizing random mixing between attendees by ending the event prior to splitting into disparate groups (Hamner et al., 2020), the proportion of people infected could have been reduced by 70 – 88% even without implementing any other intervention strategies (Fig. 4). Therefore, imposing movement restrictions could be a more effective intervention than strict duration limits.

We found that mask usage and social distancing interventions are relatively more effective for reducing proportional infection rates in small groups than in large ones. Our findings suggest that in the Skagit County choral case, duration limits with implied movement restrictions and mask usage would have been the most-effective intervention strategies for reducing SARS-CoV-2 infection rates, but multiple interventions would have needed to be deployed simultaneously to reach near-zero rates (i.e., mean rate  $< 0.5$  people / gathering duration) (Fig. 4). Infection rates generally increased with group size and decreased with mask efficacy, and we found that when movement rates were minimized (i.e., gathering durations  $\leq 40$ ) we could minimize infection rates with relatively-low mask efficacy or even no mask usage in some cases. Our results support recent evidence suggesting that even wearing masks with relatively low droplet-filtering abilities around

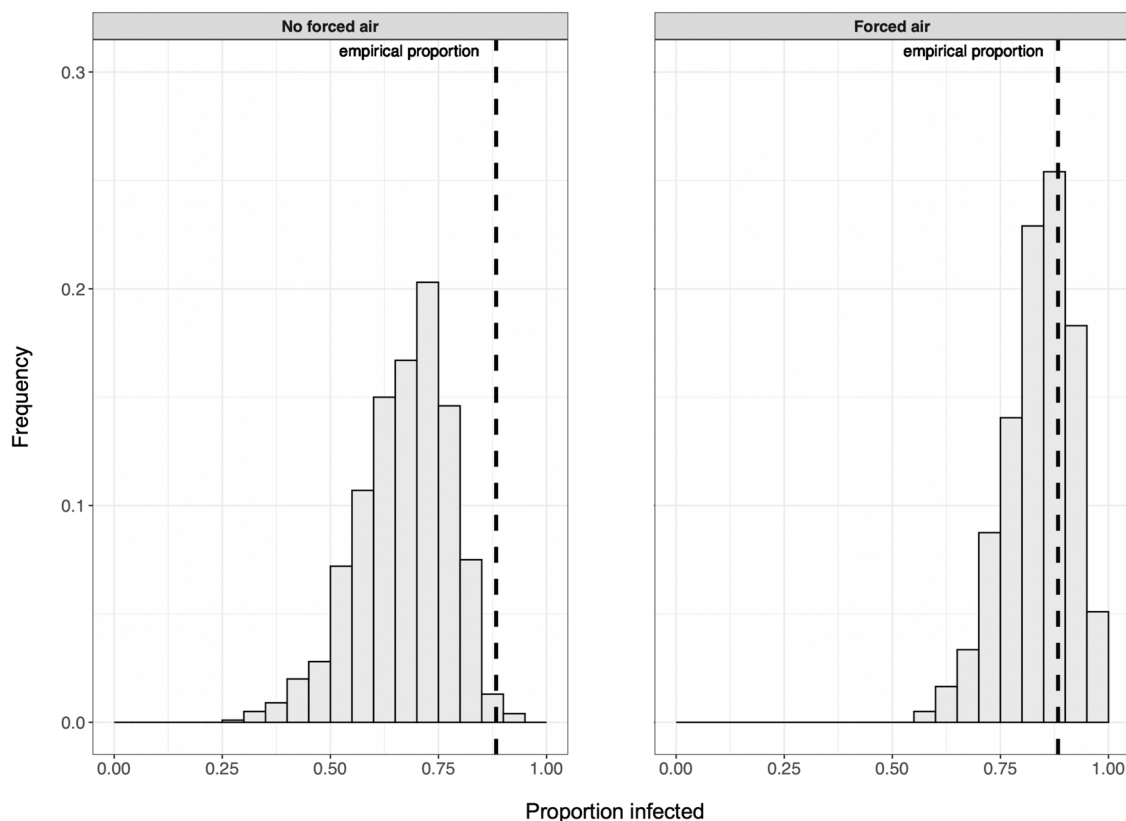


Fig. 3. In the absence of interventions to reduce transmission risk, the proportion of susceptible people infected in simulations can reflect the case study value (i.e., 0.88) and is more likely to do so when forced airflow is included.

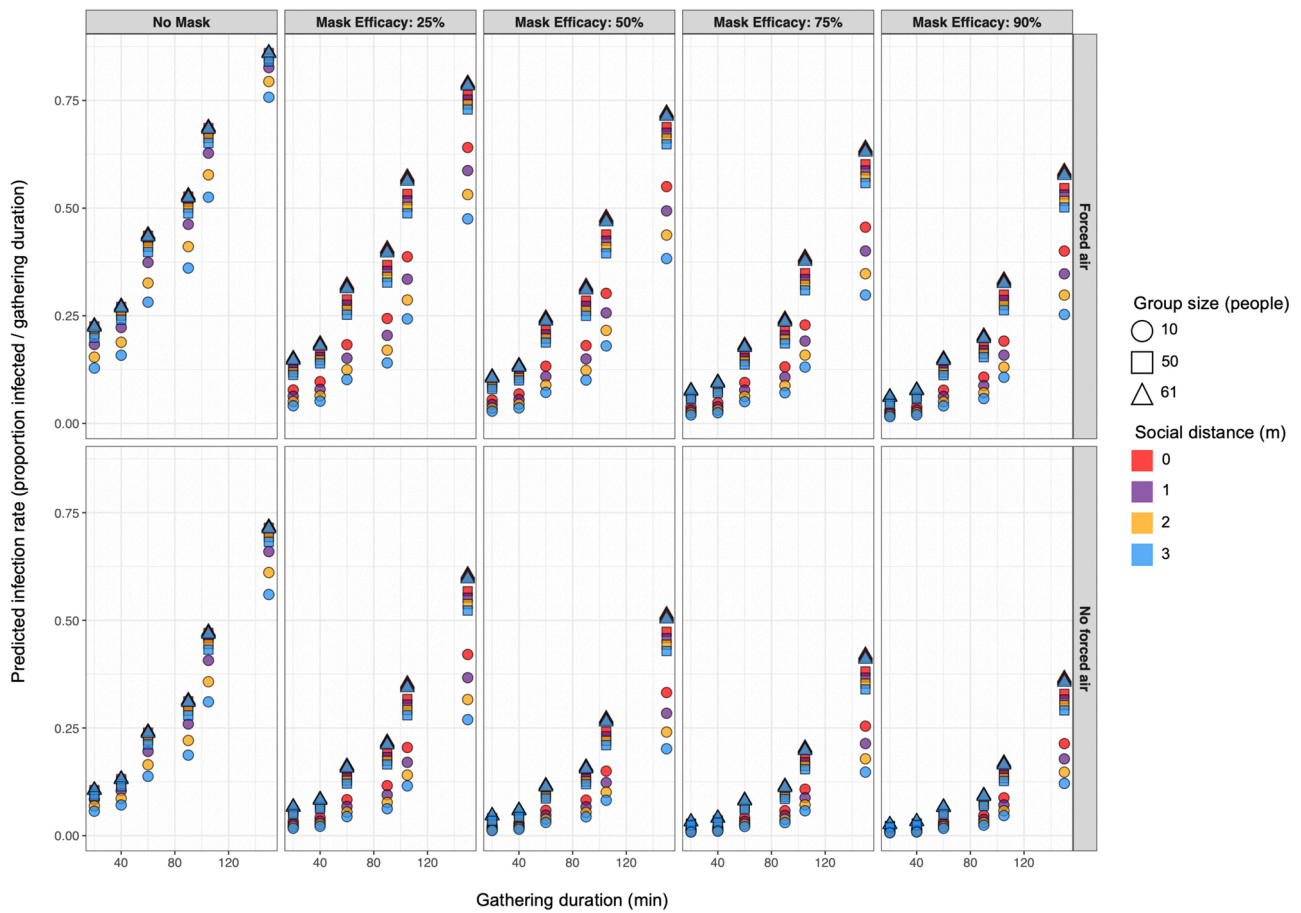


Fig. 4. Predicted mean proportion of susceptible populations infected with SARS-CoV-2 for varied parameter sets suggest that concurrent deployment of multiple interventions is required to achieve near-zero transmission rates.

Table 3

Logit scale estimates associated with 1-unit increases in covariate values given by our beta-regression model for evaluating intervention effects. Wald 95% confidence intervals are given in parentheses.

Coefficient	$\beta$ Estimate	$p$
Intercept	-2.927 (-2.940, -2.914)	-
$\phi$	5.808 (5.791, 5.824)	-
Gathering duration (min)	0.012 (0.012, 0.012)	< 0.001
Mask efficacy (%)	-0.015 (-0.015, -0.015)	< 0.001
Mask use	-0.949 (-0.964, -0.935)	< 0.001
Movement (No. rearrangements)	0.491 (0.485, 0.497)	< 0.001
Group size (people)	0.001 (0.001, 0.001)	< 0.001
Social distancing (m)	-0.250 (-0.256, -0.243)	< 0.001
Ventilation	0.898 (0.895, 0.902)	< 0.001
Mask use : Group size	0.014 (0.013, 0.014)	< 0.001
Mask use : Social distancing	-0.018 (-0.025, -0.010)	< 0.001
Group size : Social distancing	0.004 (0.004, 0.004)	< 0.001
Mask use : Group size : Social distancing	1.923e <sup>-4</sup> (3.039e <sup>-5</sup> , 3.542e <sup>-4</sup> )	0.020

others can help to reduce exposure to infectious agents (Agrawal and Bhardwaj, 2020; O’kelly et al., 2020). Attempted social distancing up to 3 m had little effect on transmission rates relative to other intervention strategies (Fig. 4). That said, because social distancing generally had a greater effect on proportional infection rates when group size was limited to 10 people, and 2-m social distances reduced the mean number of infections in larger groups, we can intuit that the relatively small overall effect of social distancing was likely due to the presence of physical barriers (e.g., edges of the simulated world) or the physical arrangement of nearby individuals impeding agents’ attempts to social distance, rather than due to far-reaching droplet spread that makes

social distancing irrelevant. This is supported by the significant interactions between the *Group size* and *Social distancing* variables, which indicate that social distancing becomes less effective at preventing secondary infections as the number of attendees increases (Table 3).

Conclusions regarding social distancing effects are further supported by our logistic regression model results that describe the relative effects of population density, gathering duration, quanta production, and ventilation on the probability of indoor SARS-CoV-2 transmission from a single infectious individual (Table 4). This model had a pseudo-R<sup>2</sup> value of 0.25 and demonstrated that among the considered variables, population density was the most-important contributor to SARS-CoV-2 transmission risk. Additionally, increases in gathering duration, infectious aerosol production, and horizontal air movement all escalate the probability that transmission will occur during gatherings, though the effect is much lesser than that of increasing population density. The relatively small effects of quanta production and duration on transmission risk suggest that once individuals are exposed to infectious media is of paramount importance for controlling COVID-19 incidence.

Regarding observed effects of ventilation in our beta and logistic regression models, our results suggest that in spite of some evidence that forced-air ventilation systems can reduce risk of respiratory pathogen infection from indoor aerosols (Escombe et al., 2007; Smieszek et al., 2019), there is potential for forced airflow to expose susceptible people to aerosolized pathogens even if they are relatively far from infectious individuals, and therefore increase transmission risk. We show that, though filtering re-circulated air can lower transmission risk (Table 4), increasing this effect is unlikely to compensate for the elevated risk

**Table 4**

Logit scale estimates associated with 1-unit increases in covariate values given by our logistic-regression model for evaluating effect on SARS-CoV-2 transmission risk during an indoor gathering. Wald 95% confidence intervals are given in parentheses.

Coefficient	$\beta$ Estimate	Odds ratio	$p$
Intercept	-0.146 (-0.151, -0.140)	-	-
Population density (people/m <sup>2</sup> )	2.766 (2.761, 2.771)	15.891 (15.813, 15.968)	< 0.001
Gathering duration (min)	0.015 (0.015, 0.015)	1.015 (1.015, 1.015)	< 0.001
Quanta (quanta/hr)	0.002 (0.002, 0.002)	1.002 (1.002, 1.002)	< 0.001
Excess droplet removal rate (%/min)	-0.024 (-0.024, -0.024)	0.976 (0.976, 0.976)	< 0.001
Air change rate (%/min)	0.017 (0.017, 0.017)	1.02 (1.02, 1.02)	< 0.001
Air filtration rate (%/min)	-0.005 (-0.005, -0.005)	0.995 (0.995, 0.995)	< 0.001

attributable to increased horizontal air-change rates (Table 3 & 4). It appears that maximizing rates of three-dimensional aerosol removal is the key to successful transmission-risk reduction when using forced-air ventilation systems as intervention tools. Our results are therefore consistent with the findings of (Bhagat et al., 2020), who advise that “displacement” ventilation systems, those designed to vertically stratify indoor air by temperature and remove warmer air, are likely able to reduce local SARS-CoV-2 transmission risk. “Mixing” ventilation systems, designed to distribute temperature and aerosols equally throughout the space, are likely insufficient for preventing transmission and may even facilitate it (Bhagat et al., 2020). Providing additional indoor airflow by opening doors/windows may reduce SARS-CoV-2 exposure risk by expediting the removal of aerosolized virions and altering the movement trajectory of these particles within the room (Ahmadzadeh et al., 2021; Pirouz et al., 2021). However, Ahmadzadeh et al. (2021) advise that individuals nearby to ventilation outlets will likely be at increased risk for exposure to aerosolized virions due to the concentration of these particles in these spaces.

Given our findings, we maintain that in areas where COVID-19 prevalence remains high, holding events associated with relatively-increased mixing rates between individuals (e.g., social gatherings, sporting events, etc.) should be avoided even if attendance rates are presumed to be low. Such events are likely to be associated with SARS-CoV-2 transmission if  $\geq 1$  infectious individual(s) were to attend, the probability of which increases linearly with group size (Chande et al., 2020). It is important to note however, that though our results provide insight into mechanisms for reducing SARS-CoV-2 transmission rates, given the effect that model parameters can have on simulation outcomes (see Appendix S3), our findings may not be reasonably extrapolated to accurately predict transmission in scenarios dissimilar from those we modeled here (e.g.,  $\geq 2$  infectious individuals, fewer aerosolized virions produced during expectorations, etc.). Regardless, we can still conclude that imposing mask usage requirements, group size restrictions, duration limits, and social distancing policies have additive, and in some cases multiplicative protective effects on individual-level SARS-CoV-2 infection risk during gatherings, and can be particularly efficacious interventions when deployed simultaneously.

A detailed list of assumptions of limitations of our ABM design can be found in the *Design Concepts* section of Appendix S1. It is worth noting that the temporal and spatial scale of our ABM (i.e., < 1 day, and within a single room) limits the applicability of our model for simultaneously simulating transmission in large populations, across separate-but-connected spaces (e.g., rooms in a house or healthcare facility, classrooms in school, etc.), and on larger time scales. However, with some modifications our ABM may be used as a base framework for models seeking to evaluate indoor pathogen transmission in these cases.

In addition to model-specific limitations, there are some simulation-related assumptions that we must acknowledge. First and foremost, all of our simulations only included a single infectious individual, and all other individuals were completely susceptible to SARS-CoV-2 infection. Given the ongoing worldwide COVID-19 vaccine rollout it is likely that at least some people attending indoor gatherings will have a level of protection from infection, and we address this further in Farthing and Lanzas (2021). The findings presented herein are still important though, because transmission to and within unvaccinated groups remains a prominent issue (Christie et al., 2021). Secondly, we simulate only limited activity-specific behaviors related to movement within indoor gatherings. For the most part, simulated individuals were unmoving and they never engaged in specific direct contact-related activities with others (e.g., hugging, close-talking, etc.) during which SARS-CoV-2 transmission risk may be elevated. This means that our simulations may oversimplify transmission mechanisms, and limits our ability to generalize our findings to specific real-world events. Nevertheless, we feel that our model is sufficiently accurate to highlight general trends in indoor SARS-CoV-2 transmission risk to susceptible populations.

#### 4. Conclusions

Our results suggest SARS-CoV-2 infections can occur quickly following exposure to infectious respiratory droplets. To maximize nonpharmaceutical intervention efficacy, we must understand and account for drivers of indoor exposure to infectious droplets and aerosols (e.g., people moving from virion-free space into contaminated areas within the room, ventilation systems pushing infectious aerosols towards susceptible individuals, etc.), so that individuals may actively take steps to avoid high-risk behaviors and environments. The ability to study these drivers is what differentiates our ABM from other models designed to study indoor SARS-CoV-2 transmission, but that do not incorporate spatiotemporal heterogeneity in agent behavior and environmental conditions.

#### Author contributions

Trevor Farthing led the model creation, data analysis, and manuscript writing. Cristina Lanzas secured the funding. Both authors conceived the ideas presented herein, contributed to model development and writing efforts, and gave final approval for publication.

#### Declarations of interest

None.

#### Acknowledgments

This work was partially supported by the Centers for Disease Control and Prevention (CDC), USA (U01CK000587-01M001) and the National Institute of General Medical Sciences, USA (R35GM134934). The funders had no role in study design, data collection and analysis, decision to publish or preparation of the manuscript. We thank Savannah Bates for providing feedback on early versions of the model. Her comments helped to improve the realism of our simulations.

#### Appendix A. Supporting information

Supplementary data associated with this article can be found in the online version at doi:10.1016/j.epidem.2021.100524.

#### References

- Adams, W.C., 1993. Measurement of Breathing Rate and Volume in Routinely Performed Daily Activities. California Air Resources Board, Sacramento, CA, USA. Final Report, Contract No. A033-205. (<https://ww2.arb.ca.gov/sites/default/files/classic/research/apr/past/a033-205.pdf>).

- Agrawal, A., Bhardwaj, R., 2020. Reducing chances of COVID-19 infection by a cough cloud in a closed space. *Phys. Fluids* 32, 101704. <https://doi.org/10.1063/5.0029186>.
- Ahmadzadeh, M., Farokhi, E., Shams, M., 2021. Investigating the effect of air conditioning on the distribution and transmission of COVID-19 virus particles. *J. Clean Prod.* 316, 128147. <https://doi.org/10.1016/j.jclepro.2021.128147>.
- Asadi, S., Cappa, C.D., Barreda, S., Wexler, A.S., Bouvier, N.M., Ristenpart, W.D., 2020. Efficacy of masks and face coverings in controlling outward aerosol particle emission from expiratory activities. *Sci. Rep.* 10, 15665. <https://doi.org/10.1038/s41598-020-72798-7>.
- Atkinson, J., Chartier, Y., Pessoa-Silva, C.L., Jensen, P., Li, Y., Seto, W.-H., 2009. Natural Ventilation for Infection Control in Health-Care Settings. World Health Organization, Geneva, Switzerland [cited 2021 Oct 03]. ([https://apps.who.int/iris/bitstream/handle/10665/44167/9789241547857\\_eng.pdf?jsessionid=1A17F4B41AC402C2746778937A854E27?sequence=1](https://apps.who.int/iris/bitstream/handle/10665/44167/9789241547857_eng.pdf?jsessionid=1A17F4B41AC402C2746778937A854E27?sequence=1)).
- Bhagat, R.K., Davies Wykes, M.S., Dalziel, S.B., Linden, P.F., 2020. Effects of ventilation on the indoor spread of COVID-19. *J. Fluid Dyn.* 903, F1. <https://doi.org/10.1017/jfm.2020.720>.
- Bourouiba, L., Dehandschoewercker, E., Bush, J.W.M., 2014. Violent expiratory events: on coughing and sneezing. *J. Fluid Mech.* 745 (2014), 537–563. <https://doi.org/10.1017/jfm.2014.88>.
- Castillo, J.E., Weibel, J.A., 2018. A point sink superposition method for predicting droplet interaction effects during vapor-diffusion-driven dropwise condensation in humid air. *Int. J. Heat Mass Trans.* 118 (2018), 708–719. <https://doi.org/10.1016/j.ijheatmasstransfer.2017.11.045>.
- Chande, A., Lee, S., Harris, M., Nguyen, Q., Beckett, S.J., Hilley, T., Andris, C., Weitz, J. S., 2020. Real-time, interactive website for US-county-level COVID-19 event risk assessment. *Nat. Hum. Behav.* 4, 1313–1319. <https://doi.org/10.1038/s41562-020-01000-9>.
- Chao, C.Y.H., Wan, M.P., Morawska, L., Johnson, G.R., Ristovski, Z.D., Hargreaves, M., Mengersen, K., Corbett, S., Li, Y., Xie, X., Katoshevski, D., 2009. Characterization of expiration air jets and droplet size distributions immediately at the mouth opening. *J. Aerosol Sci.* 40 (2), 122–133. <https://doi.org/10.1016/j.jaerosci.2008.10.003>.
- Chen, W., Zhang, N., Wei, J., Yen, H., Li, Y., 2020. Short-range airborne route dominates exposure of respiratory infection during close contact. *Build. Environ.* 176, 106859. <https://doi.org/10.1016/j.buildenv.2020.106859>.
- Christie, A., Brooks, J.T., Hicks, L.A., Sauber-Schatz, E.K., Yoder, J.S., Honein, M.A., 2021. Gaudiance for implementing COVID-19 prevention strategies in the context of varying community transmission levels and vaccination coverage. *Morb. Mortal Wkly. Rep.* 70 (30), 1044–1047. <https://doi.org/10.15585/mmwr.mm7030e2>.
- Cribari-Neto, F., Zeileis, A., 2010. Beta regression in R. *J. Stat. Soft.* 34 (2), 1–24. <https://doi.org/10.18637/jss.v034.i02>.
- Das, S.K., Alam, J., Plumari, S., Greco, V., 2020. Transmission of airborne virus through sneezed and coughed droplets. *Phys. Fluids* 32, 097102. <https://doi.org/10.1063/5.0022859>.
- van Doremalen, N., Bushmaker, T., Morris, D.H., Holbrook, M.G., Gamble, A., Williamson, B.N., Tamin, A., Harcourt, J.L., Thornburg, N.J., Gerber, S.I., Lloyd-Smith, J.O., de Wit, E., Munster, V.J., 2020. Aerosol and surface stability of SARS-CoV-2 as compared with SARS-CoV-1. *N. Engl. J. Med.* 2020 (382), 1564–1567. <https://doi.org/10.1056/NEJMc2004973>.
- Escombe, A.R., Oeser, C.C., Gilman, R.H., Navincopa, M., Ticona, E., Pan, W., Martínez, C., Chacaltana, J., Rodríguez, R., Moore, D.A., Friedland, J.S., Evans, C.A., 2007. Natural ventilation for the prevention of airborne contagion. *PLoS Med.* 4 (2), e68. <https://doi.org/10.1371/journal.pmed.0040068>.
- Farthing T., Lanzas C. When can we stop wearing masks? Agent-based modeling to identify when vaccine coverage makes nonpharmaceutical interventions for reducing SARS-CoV-2 infections redundant in indoor gatherings. Preprint. 2021. doi: 10.1101/2021.04.19.21255737.
- Ferrari, S.L.P., Cribari-Neto, F., 2004. Beta regression for modelling rates and proportions. *J. Appl. Stat.* 31 (7), 799–815. <https://doi.org/10.1080/0266476042000214501>.
- Grimm, V., Railsback, S.F., Vincenot, C.E., Berger, U., Gallagher, C., DeAngelis, D.L., Edmonds, B., Ge, J., Giske, J., Groeneveld, J., Johnston, A.S.A., Milles, A., Nabe-Nielsen, J., Polhill, J.G., Radchuk, V., Rohwäder, M.S., Stillman, R.A., Thiele, J.C., Ayllón, D., 2020. The ODD protocol for describing agent-based and other simulation models: a second update to improve clarity, replication, and structural realism. *J. Artif. Soc. Soc. Simul.* 23 (2), 7. <https://doi.org/10.18564/jasss.4259>.
- Hammer, L., Dubbel, P., Capron, I., Ross, A., Jordan, A., Lee, J., Lynn, J., Ball, A., Narwal, S., Russell, S., Patrick, D., Leibbrand, H., 2020. High SARS-CoV-2 attack rate following exposure at a choir practice – Skagit County, Washington, March 2020. *Morb. Mortal Wkly. Rep.* 69, 606–610. <https://doi.org/10.15585/mmwr.mm6919e6>.
- Jefferson, T., Foxlee, R., Del Mar, C., Dooley, L., Ferroni, E., Hewak, B., Prabhala, A., Nair, S., Rivetti, A., 2008. Physical interventions to interrupt or reduce the spread of respiratory viruses: systematic review. *Br. Med. J.* 2008 (336), 77–80. <https://doi.org/10.1136/bmj.39393.510347.BE>.
- Kwon, S.-B., Park, J., Jang, J., Cho, Y., Park, D.-S., Kim, C., Bae, G.N., Jang, A., 2012. Study on the initial velocity distribution of exhaled air from coughing and speaking. *Chemosphere* 87 (11), 1260–1264. <https://doi.org/10.1016/j.chemosphere.2012.01.032>.
- Leclerc, Q.J., Fuller, N.M., Knight, L.E., Funk, S., Knight, G.M., 2020. What settings have been linked to SARS-CoV-2 transmission clusters? *Wellcome Open Res.* 5, 83. <https://doi.org/10.12688/wellcomeopenres.15889.2>.
- Lee, K.K., Savani, A., Matos, S., Evans, D.H., Pavord, I.D., Birring, S.S., 2012. Four-hour cough frequency monitoring in chronic cough. *Chest* 142 (5), 1237–1243. <https://doi.org/10.1378/chest.11-3309>.
- Lelieveld, J., Helleis, F., Borrmann, S., Cheng, Y., Drewnick, F., Haug, G., Klimach, T., Sciare, J., Su, H., Pöschl, U., 2020. Model calculations of aerosol transmission and infection risk of COVID-19 in indoor environments. *Int. J. Environ. Res. Publ. Health* 17, 8114. <https://doi.org/10.3390/ijerph17218114>.
- Miller, S.L., Nazaroff, W.W., Jimenez, J.L., Boerstra, A., Buonanno, G., Dancer, S.J., Kurnitski, J., Marr, L.C., Morawska, L., Noakes, C., 2020. Transmission of SARS-CoV-2 by inhalation of respiratory aerosol in the Skagit Valley Chorale superspreading event. *Indoor Air* 00, 1–10. <https://doi.org/10.1111/ina.12751>.
- O'kelly, E., Pirog, S., Ward, J., Clarkon, P.J., 2020. Ability of fabric face mask materials to filter ultrafine particles at coughing velocity. *BMJ Open* 10 (9), e039424. <https://doi.org/10.1136/bmjopen-2020-039424>.
- Park, S.Y., Kim, Y.M., Yi, S., Lee, S., Na, B.J., Kim, C.B., Kim, J.I., Kim, H.S., Kim, Y.B., Park, Y., Huh, I.S., Kim, H.K., Yoon, H.J., Jang, H., Kim, K., Chang, Y., Kim, I., Lee, H., Gwack, J., Kim, S.S., Kim, M., Kweon, S., Choe, Y.J., Park, O., Park, Y.J., Jeong, E.K., 2020. Coronavirus disease outbreak in call center, South Korea. *Emerg. Infect. Dis.* 26 (8), 1666–1670. <https://doi.org/10.3201/eid2608.201274>.
- Pirouz, B., Palermo, S.A., Naghib, S.N., Mazzeo, D., Turco, M., Piro, P., 2021. The role of HVAC design and windows on the indoor airflow pattern and ACH. *Sustainability* 13 (14), 7931. <https://doi.org/10.3390/su13147931>.
- Qian, H., Miao, T., Liu, L., Zheng, X., Luo, D., Li, Y., 2020. Indoor transmission of SARS-CoV-2. *Indoor Air* 00, 1–7. <https://doi.org/10.1111/ina.12766>.
- Fryar, C.D., Kruszon-Moran, D., Gu, Q., Ogden, C.L., 2018. Mean body weight, height, waist circumference, and body mass index among adults: United States, 1999–2000 through 2015–2016. *National Health Statistics Reports*. In: No. 122. United States National Center for Health Statistics, Hyattsville, MD, USA.
- R Core Team. R: A language and environment for statistical computing. R Foundation for Statistical Computing, Vienna, Austria. (<https://www.R-project.org/>). 2020 [cited 2021 Oct 03].
- Railsback, S.F., Grimm, V., 2011. *Agent-Based and Individual-Based Modeling: A Practical Introduction*, 1st edition. Princeton University Press, Princeton, New Jersey, U.S.A., pp. 195–208.
- Riley, E.C., Murphy, G., Riley, R.L., 1978. Airborne spread of measles in a suburban elementary school. *Am. J. Epidemiol.* 107 (5), 421–432. <https://doi.org/10.1093/oxfordjournals.aje.a112560>.
- RStudio Team. RStudio: integrated development Environment for r. RStudio Team, Boston, Massachusetts, USA. (<http://www.rstudio.com/>). 2018 [cited 2021 Jan 21].
- Shao, Siyao, Zhou, Dezh, Ruichen, He, Li, Jiaqi, Zou, Shufan, Mallery, Kevin, Kumar, Santosh, Yang, Suo, Hong, Jiarong, 2021. Risk assessment of airborne transmission of COVID-19 by asymptomatic individuals under different practical settings. *J. Aerosol. Sci.* 151, 105661. <https://doi.org/10.1016/j.jaerosci.2020.105661>.
- Smieszek, T., Lazzari, G., Salathé, M., 2019. Assessing the dynamics and control of droplet- and aerosol-transmitted influenza using an indoor positioning system. *Sci. Rep.* 9, 2185. <https://doi.org/10.1038/s41598-019-38825-y>.
- Stadnyskiy, V., Bax, C.E., Bax, A., Anfunder, P., 2020. The airborne lifetime of small speech droplets and their potential importance to SARS-CoV-2 transmission. *Proc. Natl. Acad. Sci. USA* 117 (22), 11875–11877. <https://doi.org/10.1073/pnas.2006874117>.
- Sun, C., Zhai, Z., 2020. The efficacy of social distance and ventilation effectiveness in preventing COVID-19 transmission. *Sustain. Cities Soc.* 62, 102390. <https://doi.org/10.1016/j.scs.2020.102390>.
- Tjur, T., 2009. Coefficients of determination in logistic regression models – A new proposal: the coefficient of discrimination. *Am. Stat.* 63 (4), 366–372. <https://doi.org/10.1198/tast.2009.08210>.
- United States Center for Disease Control and Prevention [CDC], 2021. Scientific brief: SARS-CoV-2 and potential airborne transmission. 2020 [cited 2021 Oct 03]. (<https://www.cdc.gov/coronavirus/2019-ncov/more/scientific-brief-sars-cov-2.html>).
- Wang, C.C., Prather, K.A., Sznitman, J., Jimenes, J.L., Lakdawala, S.S., Tufecki, Z., Marr, L.C., 2021. Airborne transmission of respiratory viruses. *Science* 373 (6558). <https://doi.org/10.1126/science.abd9149>.
- Wilensky U. NetLogo. Center for Connected Learning and Computer-Based Modeling, Northwestern University, Evanston, IL. (<http://ccl.northwestern.edu/netlogo/>). 1999 [cited 2021 Oct 03].
- Wölfel, R., Corman, V.M., Guggemos, W., Seilmaier, M., Zange, S., Müller, M.A., Niemeyer, D., Jones, T.C., Vollmar, P., Rothe, C., Hoelscher, M., Bleicker, T., Brünink, S., Schneider, J., Ehmann, R., Zwirgmaier, K., Drosten, C., Wendtner, C., 2020. Virological assessment hospitalized patients with COVID-2019. *Nature* 581 (2020), 465–469. <https://doi.org/10.1038/s41586-020-2196-x>.
- World Health Organization [WHO]. *2020P. Modes of transmission of virus causing COVID-19: implications for IPC precaution recommendations: scientific brief*, 29 March 2020. <https://apps.who.int/iris/handle/10665/331616>. [accessed 12 Nov 2021].